Journal of Power Sources 229 (2013) 179–184

Contents lists available at SciVerse ScienceDirect

Journal of Power Sources

journal homepage: www.elsevier.com/locate/jpowsour

Peak utilization of catalyst with ultra-low Pt loaded PEM fuel cell electrodes prepared by the electrospray method

S. Martin, B. Martinez-Vazquez, P.L. Garcia-Ybarra*, J.L. Castillo

Dept. Fisica Matematica y de Fluidos, Facultad de Ciencias, UNED, Senda del Rey 9, 28040 Madrid, Spain

HIGHLIGHTS

- Catalytic layers with 0.01 mg_{Pt} cm^{-2} loading were generated by electrospray.
- Electrodes with 5 and 25 square centimeter active surface were prepared.
- MEAs made with these electrodes and Nafion membranes were tested in single cells.
- At atmospheric pressure and 40 °C, the MEAs deliver a specific power of 10 kW g_{Pt}^{-1}.
- At 3.4 bar gauge pressure and 70 °C, platinum utilization reached 30 kW g_{Pt}^{-1}.

GRAPHICAL ABSTRACT

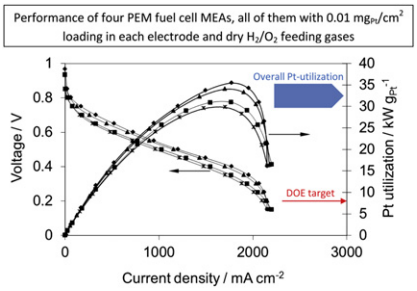

ARTICLE INFO

Article history:
Received 18 September 2012
Received in revised form
30 November 2012
Accepted 6 December 2012
Available online 13 December 2012

Keywords:
Ultra-low Pt loading
Catalytic layer
Electrospray
Electrostatic spray deposition
Electrohydrodynamic atomization
Polymeric fuel cell

ABSTRACT

The electrospray technique has been used to develop a methodology to prepare PEMFC electrodes of high performance by depositing catalytic layers with ultra-low Pt loadings – 0.01 mg_{Pt} cm^{-2} – on gas diffusion layers (GDLs) supplied with a carbon microporous layer (CMPL). The catalytic deposits exhibit a fractal structuration and good dispersion of the catalyst as they are grown by the aggregation of catalyst particles with size around 100 nm. Membrane-electrode assemblies (MEAs), made with equally loaded electrodes on both sides of the membrane, delivered performances up to roughly 600–700 mW cm^{-2} that correspond to very high overall platinum utilizations in the interval 30–35 kW g_{Pt}^{-1}. This value is about twice the largest Pt-utilization reported up to date for this kind of fuel cells.

1. Introduction

One of the major factors limiting PEM fuel cell commercialization is the amount of catalyst in the electrodes whose price represents about 30–40 % of the total cost of the fuel cell [1]. As a recognized reference, the US Department of Energy (DOE) in its Hydrogen and Fuel Cells Program Plan established the specific power per gram of platinum at 8 kW g_{Pt}^{-1} as the target for MEA performance to be achieved in the period 2017–2020 in

* Corresponding author. Tel.: +34 913986743; fax: +34 913987628.
E-mail addresses: smartin@dfmf.uned.es (S. Martin), beamar@dfmf.uned.es (B. Martinez-Vazquez), pgybarra@ccia.uned.es (P.L. Garcia-Ybarra), jcastillo@ccia.uned.es (J.L. Castillo).

0378-7753/$ – see front matter © 2012 Elsevier B.V. All rights reserved.
http://dx.doi.org/10.1016/j.jpowsour.2012.12.029

transportation applications [2]. The aim is to increase the catalyst utilization by reducing the catalyst loading of the electrodes without compromising the fuel cell performance.

Catalyst deposition by electrohydrodynamic spraying or electrospray is a suitable method to prepare nanostructured catalytic layers where the catalyst is highly dispersed with a large active surface and porosity leading to an excellent catalyst utilization [3] (for a general review on the electrospray applications, including fuel cells, see [4] and the references cited therein). The outstanding efficiency of this technique for depositing catalyst layers has been already demonstrated, especially in the range of ultra-low platinum loadings ($\leq$0.1 mg_{Pt} cm^{-2}) [5–7]. The method comprises the electro-atomization of a colloidal suspension of catalyst particles in a volatile solvent under a voltage difference between an ejector needle and a collecting substrate. The result is a nearly monodisperse spray of charged droplets of solvent, each of them carrying some catalyst particles, and emerging from a Taylor-cone formed at the needle tip [8]. The main advantage of the electrospray comes from its electrical nature. During the flight from the nozzle to the collector, the charge of the droplets prevents coagulation and moreover, as the solvent of the droplets evaporates, the imbalance between surface tension and electrostatic forces reaches a critical value (Rayleigh limit) that causes the appearance of a Taylor-cone-like deformation on the droplet surface through which the droplet discharges by emitting smaller charged micro-droplets (a phenomenon referred commonly as Coulomb fission or explosion) [9]. If the droplet flight time is long enough (*i.e.*, the needle–substrate distance is large enough), this process continues until the solvent of the droplets evaporates completely leaving dry catalyst particles which may deposit on the substrate. Consequently, each droplet evolves from the micrometric size when the spray is formed at the nozzle down to the dry residue (particles of nanometric size) near the substrate. This technique offers other remarkable benefits. On the one hand, the experimental set-up is inexpensive and simple, as only requires a high voltage power supply and a pump-needle system. On the other hand, the scale-up process is as easy as to increase the needle–substrate distance and use suitable masks of a dielectric material for focusing purposes onto the required size. By following all the above guidelines, a new methodology has been developed that allows preparation of controlled nanostructured catalyst layers with ultra-low Pt loadings down to 0.01 mg_{Pt} cm^{-2} (patent pending [10]).

In the present work, the remarkable performance of these catalytic layers have been enhanced by adding the well-known benefits provided by gas diffusion layers (GDLs) coated with a microporous layer of carbon nanoparticles (CMPL). The resulting electrodes are used to prepare membrane electrode assemblies (MEAs) with Nafion® 212 membranes. The performance of these MEAs are tested in a commercial single cell hardware.

Summarizing, two main features differentiate the activities reported here from our previous works with the electrospray deposition method. First, the same ultra-low electrosprayed Pt-loading was applied in both electrodes (instead of only in the cathode as it was done in our previous works). And second, GDLs with a carbon microporous layer were used, also in both electrodes. Furthermore, the range of operational conditions has been enlarged and the electrode size scale-up from 5 cm^2 to 25 cm^2 has been successfully achieved, together with the influence of the hot-pressing in the assembling process and the use of air, rather than oxygen, as feeding gas.

2. Experimental

Catalyst inks to be electrosprayed were prepared by mixing Pt/C powder (Pt 10 wt.% on Vulcan XC-72R) as catalyst, ethanol (96% v/v, Panreac) as solvent and Nafion® (Aldrich, 5wt.% in lower aliphatic alcohols and water) as ionomer. Based on the optimization analysis of Nafion® loading (weight percentage in the deposited solids) for ultra-low Pt loadings carried out in a previous study [6], a Nafion® loading of 50% was selected here. The concentration of the catalyst ink was taken as 7.5 mg Pt/C per ml of ethanol because the resulting suspension can be electrosprayed stably [11]. Prior to its electrospray ejection, the catalyst ink was subjected to ultrasonic stirring during 2 h with a polymeric surfactant for dispersing the Pt/C catalyst particles.

The gas diffusion layer (GDL) was commercial TORAY® carbon paper coated with a carbon microporous layer (CMPL) on one side (TP-CMPL Electrochem, Inc.). Electrodes with a Pt loading of 0.01 mg_{Pt} cm^{-2} were prepared by electrospraying the catalyst ink on the GDL with the carbon microporous layer facing the ejector needle. The electrospraying parameters, according to the electrospray experimental set-up described in [6,7] were: a needle-substrate distance of 7 cm, an electrospraying flow-rate of 0.2 ml h^{-1} and a voltage difference between the needle and the substrate in the range of 9 kV.

These electrodes were used to assemble MEAs with a 5 cm^2 active surface. Each MEA consisted of a Nafion® 212 membrane (Electrochem, Inc.) inserted between two electrodes (cathode and anode) with the same Pt loading of 0.01 mg_{Pt} cm^{-2} on each electrode. In most cases, the three components of the MEAS were directly sandwiched between the gas distributor plates. For comparison, in some cases the MEAs were subjected to a hot-pressing step to bond the electrodes and the membrane.

The electrochemical performance of the MEAs was evaluated by the current–voltage characteristic curves. A commercial fuel cell hardware (Electrochem, Inc.) connected to an external electronic load (Hocher & Hackl ZS506) was used to obtain the polarization curves. The current–voltage characteristics of the different MEAs were acquired with dry feeding gases (H_2 in the anode and O_2 or synthetic air on the cathode). The mass flows were chosen to achieve self-humidification conditions at each point of the polarization curve [7,12]. Data were collected once the cell voltage achieved a stable reading. Measurements were performed at two different temperatures, 40 °C and 70 °C, and two different pressures, ambient pressure and a gauge pressure of 3.4 bar set by back-pressure regulators. Moreover, a partial characterization by electrochemical impedance spectroscopy (EIS) was also accomplished with a frequency response analyzer coupled to a potentiostat/galvanostat (Autolab PGSTAT302N). The analysis was carried out at a cell voltage of 0.7 V with amplitude of the AC signal of 10 mV in the frequency range of 1 Hz–50 kHz.

Moreover, to test the dependence of MEA performances on scaling-up, MEAs with 25 cm^2 active surface were also prepared by setting the electrospraying parameters to the following values. Needle-substrate distance: 11 cm, electrospraying flow-rate: 0.2 ml h^{-1} and voltage difference between the needle and the substrate around 12 kV. Polarization curves of these larger MEAs were also obtained and compared with those for the 5 cm^2 MEA curves.

Finally, the morphology of the catalyst layers was examined by using a scanning electron microscope (SEM Hitachi S-3000N). To enhance the quality of the images, the samples were coated with an Au–Pd alloy (Polaron Range SC7620 sputter-coater instrument).

3. Results and discussion

3.1. Characterization of the catalyst layer

Fig. 1 displays the morphology of the catalyst layer prepared with a Pt loading of 0.01 mg_{Pt} cm^{-2} deposited by electrospray over

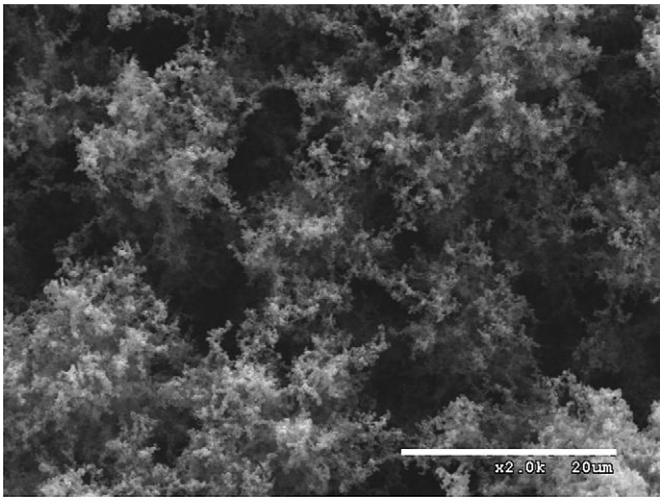

a)

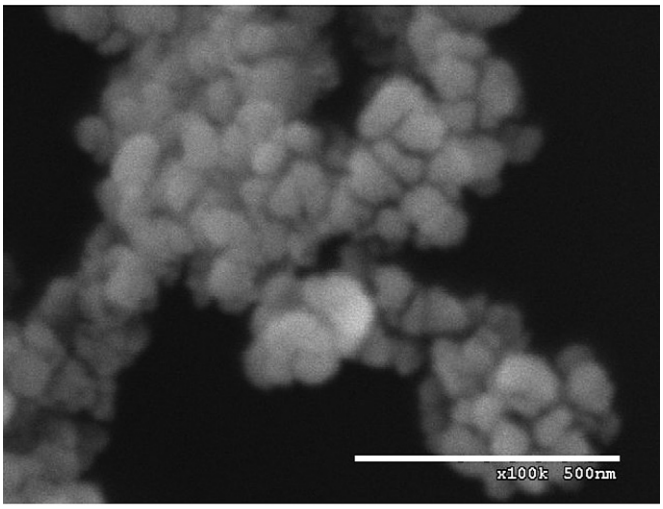

b)

Fig. 1. a) SEM micrograph of the catalytic layer with a Pt loading of 0.01 mg_{Pt} cm^{-2} deposited by electrospray. b) Enlarged view of a single dendrite. The horizontal bar is 20 μm length in a) and 500 nm in b).

the substrate (carbon paper with CMPL). The catalytic layer is conformed by fractal-like structures which have grown up from the aggregation of individual clusters (of a few catalyst particles each) with a characteristic size of 100 nm forming dendritic arrangements. The small size of the catalyst clusters causes that most of the catalyst remains exposed to the reactant gas, yielding a huge increase of the effective catalytic active surface. Besides, the fractal assembly of the catalyst clusters results in a deposit with enhanced permeability.

Fig. 2 shows a cross-section of the GDL with the electrosprayed catalytic layer deposited on the top. The profile of the catalytic layer exhibits a rather uniform thickness (∼50 μm) that is well-preserved throughout the electrode surface. The porosity of this deposit has been estimated as the proportion of the void volume to the total volume of the catalytic layer [5,13] resulting a value close to 98%. This high porosity, which can be achieved by the electrospray method due to the electric charge and the small size of the catalyst particles, reinforces the high dispersion of the catalytic material and it is a crucial factor to achieve a large Pt utilization. For comparison, substantially smaller porosity values of 60% and 30%

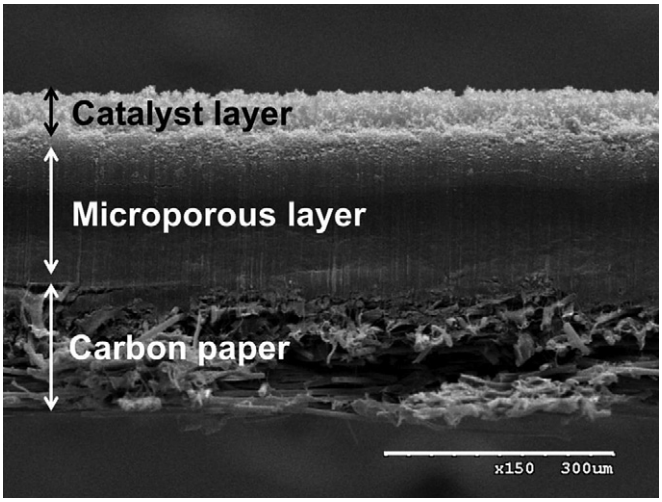

Fig. 2. Cross-sectional SEM micrograph of the electrode with a Pt loading of 0.01 mg_{Pt} cm^{-2}. The horizontal bar is 300 μm length.

have been reported in the literature for the decal [13] and the airbrush spray technique [14] respectively.

The morphology of the CMPL that supports the electrosprayed catalyst layer is presented in Fig. 3. The building blocks of the CMPL are carbon nanoparticles with a characteristic size of the same order as the electrosprayed catalyst particles (∼100 nm). When using the electrospray deposition method, two main advantages arise from this type of support for the catalyst layer with respect to the standard gas diffusion layer based on carbon fiber paper or carbon cloth. On the one hand, the depositing electrosprayed particles extend over the entire surface instead of being restricted to the outermost fibers of the gas diffusion layer. The reason is related to the electric field strength near the substrate. When the substrate is a smooth surface, the electric field lines are evenly distributed over the surface (except for a small region near the border) and the electrosprayed particles may equally deposit in any location of the substrate surface. However, when the substrate is formed from carbon fibers, these fibers focuses the electric field strength in its vicinity acting as local attractors for the electrosprayed particles and leaving void spaces between them [6,7].

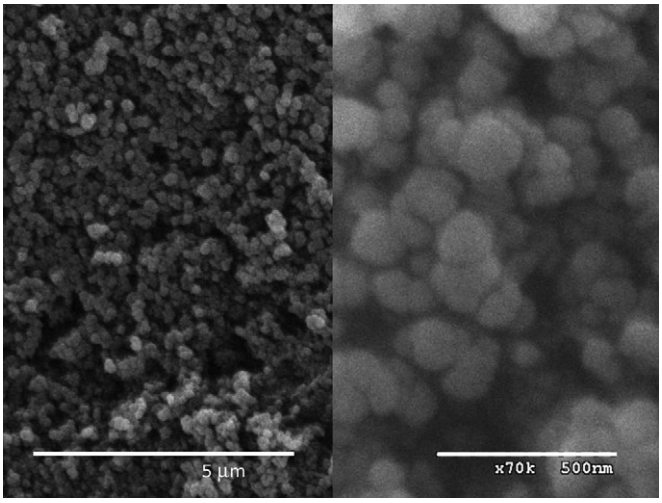

Fig. 3. SEM images of the carbon microporous layer that supports the catalytic layer. The horizontal bar in the left and the right image is 5 μm and 500 nm in length respectively.

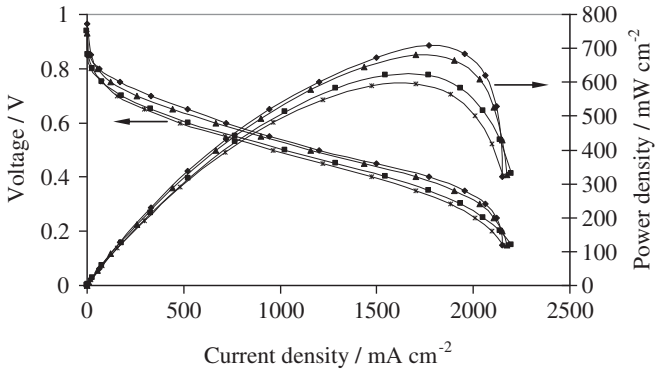

Fig. 4. Current–voltage characteristics and power density curves corresponding to MEAs whose electrodes were prepared under the same electrospraying parameters with a Pt loading of 0.01 mg_{Pt} cm^{-2} in each electrode. All measurements were carried out with dry (non-humidified) H_2/O_2, back-pressure of 3.4 bar and temperature of 70 °C.

Therefore, there is a significant increase in the deposited surface when depositing over CMPL with respect to carbon paper or carbon cloth. Another benefit of the CMPL is that the size of the carbon particles is similar to the size of the electrosprayed catalyst particles. Thus, the contact surface between the catalytic layer and the gas diffusion layer is maximized, whose effect being to reduce the electrical contact resistance and to facilitate the water drainage.

3.2. Electrochemical fuel cell performance

Fig. 4 shows the current–voltage characteristics and the power density curves of four MEAs with 5 cm^2 active surface electrodes. All these electrodes were prepared under the same experimental conditions, according to the methodology explained above, with the same final Pt loading, 0.01 mg_{Pt} cm^{-2}. The maximum performance of the MEAs falls in a relatively narrow range that extends roughly from 600 to 700 mW cm^{-2} showing up the degree of reproducibility of the deposition methodology. The most important parameter is the high platinum utilization achieved by these electrodes. Thus, from the maximum power density data, an overall specific power between 30 and 35 kW g_{Pt}^{-1} is inferred (the overall 0.02 mg_{Pt} cm^{-2} for the whole MEA was considered to measure this overall Pt-utilization). To the best of our knowledge, these figures denote the maximum platinum utilization reported in the literature for any catalyst deposition method. In fact, these results overcome in more than 50% the highest specific power actually reported [15] and represents an increase in more than 3 times respect to our previous work [7], where only the cathode was prepared by electrospraying and carbon paper was used as substrate (without CMPL).

Table 1
Ohmic resistance and charge transfer resistance corresponding to the MEAs of Fig. 4 calculated from the impedance spectra of Fig. 5.

Power density/mW cm^{-2}	R_Ω/Ω cm^2	R_{ct}/Ω cm^2
709	0.27	0.55
680	0.24	0.65
619	0.24	0.79
596	0.26	0.86

The impedance spectra corresponding to the MEAs of Fig. 4 at low overpotentials (0.7 V) are depicted in Fig. 5. For all MEAs, the Nyquist plot responds closely to a simple Randles circuit. The single impedance arc indicates that at such a low overpotential (low current density) the electrochemical process is driven by the interfacial kinetics of the oxygen reduction reaction (ORR) at the cathode and no transport limitations occur [16]. Furthermore, the good fitting of the single arc by a semicircle points toward a well-defined capacitive time constant which is usually associated, in one way or another, to a negligible roughness of the electrode surface [17,18].

The overall ohmic resistance R_Ω (sum of the electronic, ionic and contact resistance in all the components of the fuel cell) is given by the high-frequency intercept of the impedance arc with the real axis whereas the diameter of the arc is related to the charge transfer resistance R_{ct} in the cathode–electrolyte interface. The ohmic resistance and the charge transfer resistance obtained from the Nyquist plots of Fig. 5 are presented in Table 1. These results show that all the MEAs have very similar ohmic resistances. Note that the same electrospraying parameters were used in the preparation of the catalyst layers so the catalytic layer morphology was much alike in all these MEA. Therefore, a similar ohmic resistance is expected since the GDL, the membrane and the test fuel cell hardware were the same in all the cases. Moreover, it is noteworthy to point out that this high-frequency intercept occurs with a very large slope, which corresponds to a catalytic layer with planar (not porous) form without any clear sign of 45° straight line behavior [19].

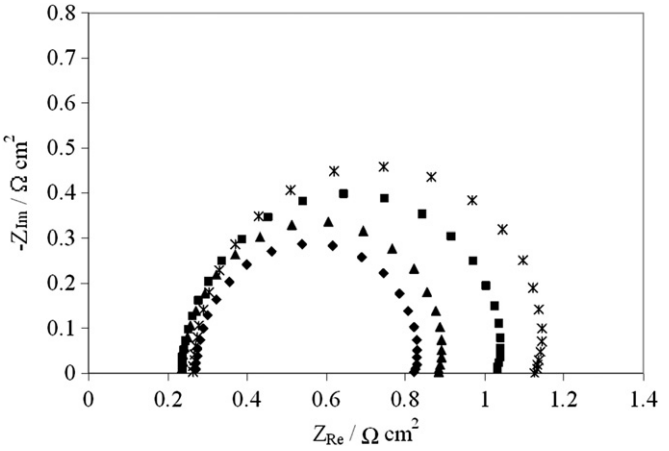

Fig. 5. Impedance spectra at a cell potential of 0.7 V corresponding to the MEAs of Fig. 4. All measurements were carried out with dry (non-humidified) H_2/O_2, back-pressure of 3.4 bar and temperature of 70 °C.

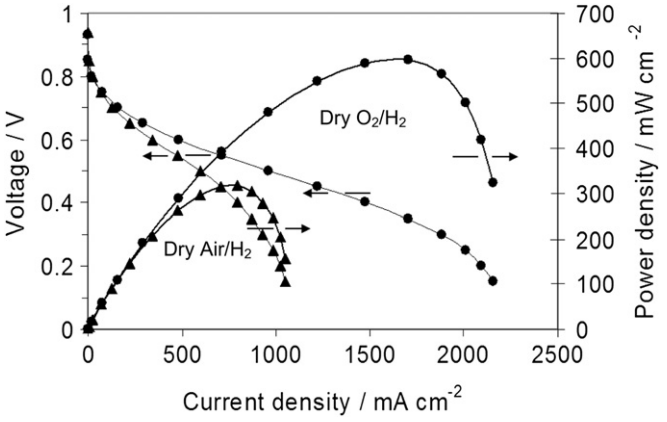

Fig. 6. Current–voltage characteristics and power density curves corresponding to one of the MEAs of Fig. 4 when is operated with: ● – dry oxygen, ▲ – dry air. The cell was tested at a temperature of 70 °C and a back-pressure of 3.4 bar.

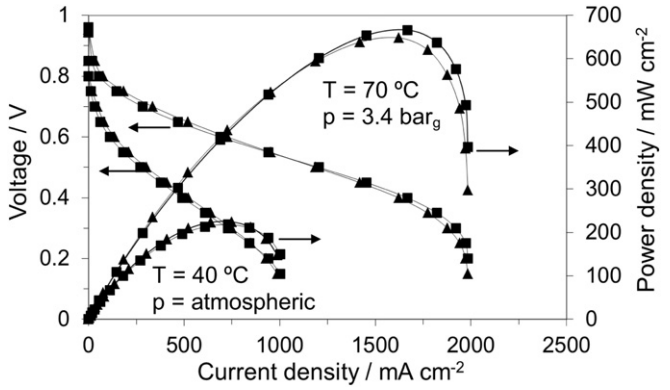

Fig. 7. Current–voltage characteristics and power density curves obtained under different (pressure and temperature) operating conditions, as labeled. In all cases, the feeding gases were dry H_2/O_2. Each electrode was prepared with a 5 cm^2 active area and a Pt loading of 0.01 mgPt cm^{-2}by electrospraying the catalyst on: ■ – membrane, ▲ – CMPL. The MEAs were assembled by hot pressing.

In contrast with the similar values of the ohmic resistances, the results of Table 1 show larger fluctuations in the values of the charge transfer resistance among the four MEAs with mutual relative deviations of about 10%. These fluctuations reflect the differences in the electrochemical kinetics of the electrodes which may be caused by the inherent randomness associated to the deposition of the catalyst particle aggregates that finally accommodates the electrode–electrolyte interface. The impedance spectra are consistent with the performances obtained for the MEAs in Fig. 4 since the greater the charge transfer resistance the poorer the ORR kinetics and hence the lower the performance.

Fig. 6 is a comparison between the performances of one of the MEAs in Fig. 4 fed with air and with pure oxygen. The use of pure oxygen entails an increase of its partial pressure and the fuel cell thermodynamics is enhanced. The ratio of the maximum performances in the two cases is 1/1.88, what is about twice larger than the value of the ratio of the partial pressures of oxygen in the corresponding feeding gases, around 1/4.

The beneficial effect of increasing the overall pressure and temperature operation conditions on the fuel cell performance is shown in Fig. 7 [20]. The same figure shows also the small differences that result by electrospraying the catalyst on the CMPL of the electrode or on the membrane. In these cases, the MEAs were assembled by hot pressing.

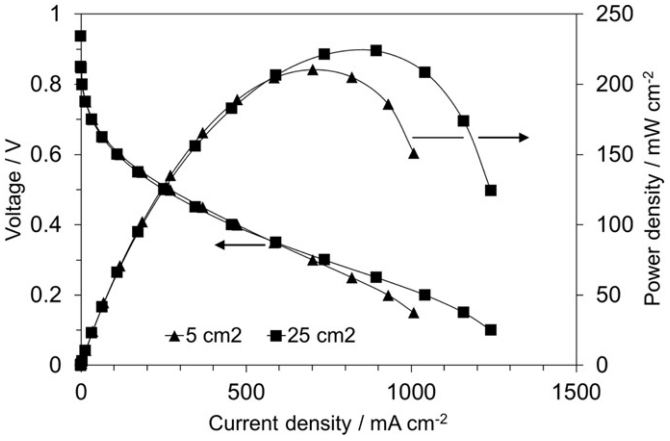

Fig. 8. Comparison of the current–voltage characteristics and power density curves obtained with MEAs with the same Pt loading of 0.01 mgPt cm^{-2} in each electrode but with different active area: ▲ – 5 cm^2 ■ – 25 cm^2. In both cases, the cells were fed with dry H_2/O_2 and the operating conditions were 40 °C and atmospheric pressure.

Finally, the endurance of the MEAs performance on scaling-up is shown in Fig. 8 by comparing MEAs with two different active areas, 5 cm^2 and 25 cm^2. In both cases, the cells were fed with dry H_2/O_2 working at 40 °C and atmospheric pressure.

4. Conclusions

A deposition methodology has been developed, based on deposition by electrospray [10], which allows the preparation of nano-structured catalytic layers with ultra-low Pt loadings and uniform thickness over any area in the range usually required by PEM fuel cell electrodes. MEAs of two different sizes were implemented from commercial GDLs of carbon paper coated with a microporous layer of carbon nanoparticles (CMPL). Catalytic inks prepared as colloidal suspensions of Pt/C nanoparticles (10% weight) in diluted Nafion® - ethanol solutions were electrosprayed on the CMPLs over two different active areas of 5 and 25 cm^2 to generate catalytic layers with Pt loadings of 0.01 mg$_{Pt}$ cm^{-2}. Each size was prepared under the same electrospraying parameters to allow the comparison under different operating conditions. At atmospheric pressure and 40 °C, the MEAs were able to deliver a power density around 200 mW cm^{-2} that corresponds to an overall specific power of about 10 kW g_{Pt}^{-1}, a figure larger than the target proposed by the US DOE for the period 2015–2020 (8 kW g_{Pt}^{-1} in transportation applications [2]). Moreover, under more suitable working conditions, at 3.4 bar of gauge pressure and 70 °C, the overall platinum utilization reached values larger than 30 kW g_{Pt}^{-1}. Such a dramatic increase of the platinum utilization, to our knowledge the highest reported in literature, is attributed to the deposition methodology that enables a high dispersion of the catalyst particles in a dendritic arrangement of small clusters that are deposited over a CMPL of nanoparticles with the same characteristic size (around 100 nm). In fact, this kind of deposition process of charged nano-particles results from the combination of a systematic particle drift toward the deposit, due to the electric field between the needle and the collector, and a particle random displacement induced by the inter-particle Coulombian interaction and to the roughness of the deposit surface. The fractal structure of these kind of deposits was analyzed in [21,22] and, among other characteristics, it implies a continuous distribution of the pore sizes covering the whole range of allowed lengths. The macropore scale is dictated by the layer height whereas the nanoparticle interspace defines the microporosity scale. The advantages of this type of morphological structuration have been recently stressed in [23] where the benefits of a fractal channel distribution of the gas supply and water outlet systems, as well as the inclusion of differentiated macro and nano-porosity in the catalytic layer of a PEMFC is shown to improve the energy efficiency and to save catalyst material.

A comparative study of the electrochemical impedance of the MEAs characterized in Fig. 4 has been accomplished by standard EIS analysis. The Nyquist plots of the EIS spectra, performed in the low overvoltage region, agree with the behavior of a planar electrode (i.e., negligible electrolyte resistance of the catalytic layer and insignificant roughness) which suggests that only the smallest scales of the initial fractal structures survive in the catalytic layer after the compression step of the MEA assembling process. Also, the ohmic resistance and the charge transfer resistance of the four MEAs were obtained from the impedance analysis. A total ohmic resistance, close to 0.25 Ω cm^2 for all MEAs, was deduced. This common value turns out to be relatively higher than expected, probably as a consequence of the operation with dry gases. Under drying conditions the fuel cell is prone to undergo undesirable unsteady behavior [24,25] and research is underway with humidified feeding gases to circumvent this possible problem and to

optimize the power delivery. On the other hand, the values of the charge transfer resistance show variations among the different sample MEAs with a typical relative deviation of around 10% that seems to be an intrinsic ingredient of this methodology. Extension of the impedance analysis under conditions of medium and large overvoltage operation is ongoing. Results will be published in a forthcoming publication.

Acknowledgments

This work has been supported by the Ministerio de Economía y Competitividad (Spain) under Grant ENE2011-26868 and Program Consolider-Ingenio 2010 (CSD2010-00011) and also by Comunidad de Madrid (Project HYSYCOMB, S2009ENE- 1597).

References

[1] J.-H. Wee, K.-Y. Lee, S.H. Kim, J. Power Sources 165 (2007) 667–677.
[2] The Department of Energy, Hydrogen and Fuel Cell Program Plan. p. 3.4–27 (September 2011).
[3] S. Martín, D. Galán, D. Rodríguez-Pérez, I.G. Loscertales, J.L. Castillo, A. Barrero, P.L. García-Ybarra, in: W. Maenhaut (Ed.), Proceedings of the European Aerosol Conference, Ghent, Belgium, 2005, p. 637.
[4] A. Jaworek, A.T. Sobczyk, J. Electrost. 66 (2008) 197–219.
[5] O.A. Baturina, G.E. Wnek, Electrochem. Solid-State Lett. 8 (2005) A267–A269.
[6] S. Martin, P.L. Garcia-Ybarra, J.L. Castillo, J. Power Sources 195 (2010) 2443–2449.
[7] S. Martin, P.L. Garcia-Ybarra, J.L. Castillo, Int. J. Hydrogen Energy 35 (2010) 10446–10451.
[8] G.I. Taylor, Proc. R. Soc. London A 280 (1964) 383–397.
[9] A. Gomez, K. Tang, Phys. Fluids 6 (1994) 404–414.
[10] P.L. Garcia-Ybarra, J.L. Castillo, S. Martin, Patent Application No. P201200341.
[11] S. Martin, A. Perea, P.L. Garcia-Ybarra, J.L. Castillo, J. Aerosol Sci. 46 (2012) 53–63.
[12] C.J.M. Janssen, M.L.J. Overvelde, J. Power Sources 101 (2001) 117–125.
[13] H.A. Gasteiger, W. Gu, R. Makharia, M.F. Mathias, B. Sompalli, in: W. Vielstich, A. Lamm, H.A. Gasteiger (Eds.), Beginning-of-life MEA Performance-Efficiency Loss Contributions, John Wiley and Sons Ltd, Chichester, 2003, pp. 593–610.
[14] J. Ihonen, F. Jaouen, G. Lindbergh, A. Lundblad, G. Sundholm, J. Electrochem. Soc. 149 (2002) A448–A452.
[15] M. Cavarroc, A. Ennadjaoui, M. Mougenot, P. Brault, R. Escalier, Y. Tessier, J. Durand, S. Roualdes, T. Sauvage, C. Coutanceau, Electrochem. Commun. 11 (2009) 859–861.
[16] X. Yuan, H. Wang, J.C. Sun, J. Zhang, Int. J. Hydrogen Energy 32 (2007) 4365–4380.
[17] R. de Levie, J. Electroanal. Chem. Interfacial Electrochem. 261 (1989) 1–9.
[18] T. Pajkossy, J. Electroanal. Chem. 364 (1994) 111–125.
[19] A. Lasia, J. Electroanal. Chem. 397 (1995) 27–33.
[20] J. Zhang, H. Li, R.J. Zhang, ECS Trans. 19 (2009) 65–76.
[21] D. Rodriguez-Perez, J.L. Castillo, J.C. Antoranz, Phys. Rev. E 72 (2005) 021403.
[22] D. Rodriguez-Perez, J.L. Castillo, J.C. Antoranz, Phys. Rev. E 76 (2007) 011407.
[23] S. Kjelstrup, M.-O. Coppens, J.G. Pharoah, P. Pfeifer, Energy Fuels 24 (2010) 5097–5108.
[24] D.G. Sanchez, D. Guinea Diaz, R. Hiesgen, I. Wehl, K.A. Friedrich, J. Electroanal. Chem. 649 (2010) 219–231.
[25] D.G. Sanchez, P.L. Garcia-Ybarra, Int. J. Hydrogen Energy 37 (2012) 7279–7288.